Eidgenössische
Technische Hochschule
Zürich

Ecole polytechnique fédérale de Zurich
Politecnico federale di Zurigo
Swiss Federal Institute of Technology Zurich

Institut für Integrierte Systeme

Integrated Systems Laboratory

Charge Carrier Quantization Effects in Double-Gated SOI MOSFETs

Andreas Wettstein, Andreas Schenk, Andreas Scholze,
Gilda Garretón, and Wolfgang Fichtner

Technical Report No. 97/6

October 1997

Abstract

Double-gated SOI devices are widely recognized as candidates for further down-scaling of MOSFETs. It has been suggested to reduce their low sensitivity to short channel effects even further by using differently doped front and back poly gates [1]. Here, we numerically investigate the influence of charge carrier quantization on the threshold voltage in these narrow channel devices comparing equally against differently doped poly gates.

Presented at:

Spring Conference of the Electrochemical Society, Inc., Montréal, May 9, 1997

1 Introduction

Quantum-mechanically, carriers are not point particles but waves of some nonzero extension. If device dimensions are scaled down to lengths comparable to this extension, the wave nature of the carriers cannot be neglected anymore as is done in classical device simulations by using a local relationship between density, quasi Fermi potential, and electrostatic potential. In silicon the wavelength of an electron of room temperature kinetic energy is about 8 nm (assuming motion along the longitudinal axis of the cigar-shaped isoenergy surface). Thus, for ultra-thin SOI MOSFETs like the double-gated device sketched in Fig. 1, quantization has to be taken into account.

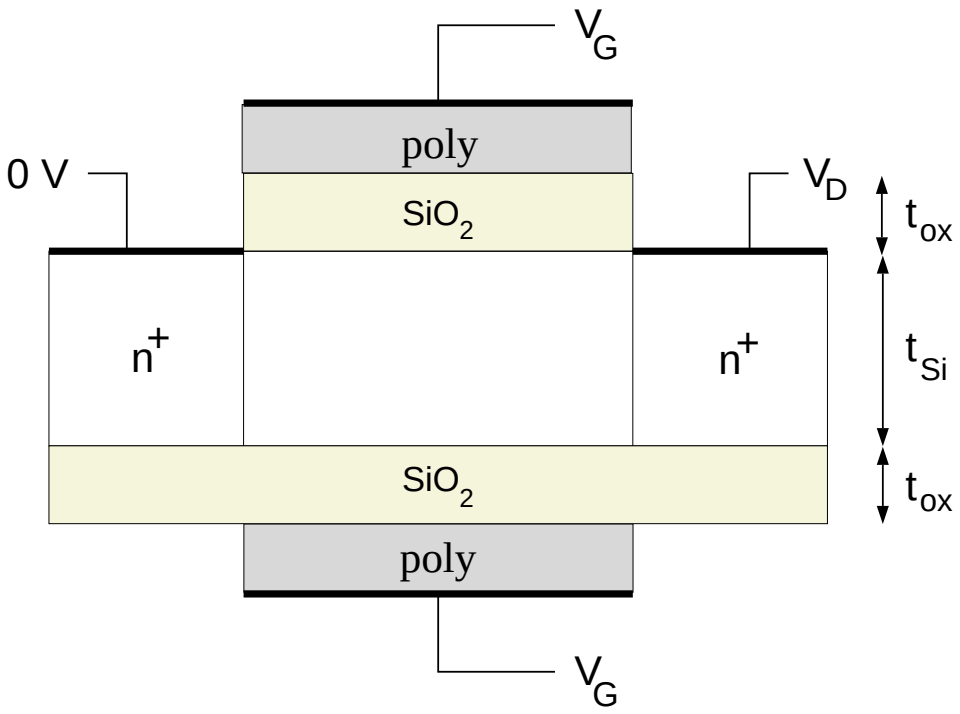

Figure 1: Model of the double gated SOI MOSFET used in our calculations.

Due to the wave nature of the carriers, the density at the oxides does not jump from some finite value to zero at once, but changes more slowly. This leads to a modified charge distribution that is shifted away form the oxides, and depends on the potential in a nonlocal way. Additionally, and most importantly, because of the extension of the wave, a carrier cannot reside precisely in the minimum of the potential, but also "feels" the higher potential in the neighborhood. Therefore, the energy will be larger than expected classically, and thus the charge density will be lower. The modified charge density will act back on the potential. At the same gate voltage the classical theory overestimates the density (see Figs. 2 and 3). To reproduce this density, the gate voltage must be significantly higher than expected classically. In the simulations of the IV characteristics this shows up as an increase in the threshold voltage (see Figs. 4 and 5).

2 Physical model

2.1 1D Schrödinger equation in effective mass approximation

In direction perpendicular to the Si-SiO_2 interfaces, the carriers are described by a one dimensional Hamiltonian in effective mass approximation,

$$H^\nu = -\frac{\partial}{\partial z}\frac{\hbar^2}{2m_z^\nu(z)}\frac{\partial}{\partial z} + V(z). \tag{1}$$

ν labels the various conduction or hole band valleys. The potential V is the sum of the electrostatic potential and the band edge energies of the material. The former has to be calculated self-consistently from the charge density.

$m_z^\nu(z)$ is the effective mass component for motion in z-direction. For electrons in Si it is given by

$$1/m_z^\nu = \sum_{i=1}^{3} z_i^2/m_i^\nu, \tag{2}$$

where the m_i^ν are effective masses on main axes and z_i are components of the unit vector $\vec{e}_z$ pointing in z-direction. The numerical values taken for m_i^ν are the ones proposed by Green [2]. For holes, we consider a heavy and a light hole band and use the formula for the warped energy surfaces of holes,

$$1/m_z^{l,h} = 1/m^{l,h}\left(\vec{e}_z\right) = A \pm \sqrt{B^2 + C^2(z_1^2 z_2^2 + z_2^2 z_3^2 + z_3^2 z_1^2)}, \tag{3}$$

where we use the parameters given by Lawaetz [3].

The 1D treatment is adequate as long as the changes in the other directions occur on length scales larger than the phase coherence length of the carriers, which is about 20 nm for electrons in Si at 300 K [4].

In our 1D treatment, the system is assumed to be homogeneous in the xy-plane. Still, m_x and m_y are functions of z. Handling this dependence correctly requires an additional potential term in Eq. (1) that depends on z and the momentum p_{xy} in the xy-plane. We neglect the z-dependence of this term. As the value of the wave function in the oxides is small, this approximation will not affect the eigenenergies and the wave functions in the silicon region too much.

2.2 Computing the charge density

Having obtained all i_{max} eigensolutions $H^\nu\Psi_i^\nu = E\Psi_i^\nu$ up to an energy E_{max} for all valleys, the quantum-mechanical contribution to the charge density (using Maxwell statistics) is computed as

$$\begin{aligned} n^{qm}(z) &= \frac{kT}{\pi\hbar^2}\sum_\nu m_{xy}^\nu(z)\sum_{i=1}^{i_{max}}|\Psi_i^\nu(z)|^2 \times \\ &\quad \left[\exp\left(\frac{E_f - E_i^\nu}{kT}\right) - \exp\left(\frac{E_f - E_{max}^\nu}{kT}\right)\right], \end{aligned} \tag{4}$$

(For Fermi statistics, $\exp x$ is replaced by $\log[1+\exp x]$), where E_f is the quasi Fermi potential and $m_{xy}^{\nu} = \sqrt{m_x^{\nu} m_y^{\nu}}$ is the effective mass for the motion in the xy-plane. For electrons, the latter can be computed analogous to m_z^{ν} in Eq. (2). For holes, we apply

$$\tilde{m}_{xy}^{l,h} = \frac{1}{2\pi} \int_0^{2\pi} d\phi m^{l,h} \left(\vec{e}_x sin\phi + \vec{e}_y cos\phi \right),$$

with the functions $m^{l,h}(\vec{e}_z)$ given by Eq. (3). The parameters used in Eq. (3) are intended for $T = 0$. Due to the very strong non-parabolicity of the hole bands, the density of state mass computed from these parameters is much smaller than the value for $T = 300\,\mathrm{K}$. Therefore, we set

$$m_{xy}^{l,h} = \tilde{m}_{xy}^{l,h} \frac{m_{DOS}^{3/2}}{\tilde{m}_{xy}^{l} \sqrt{m_z^l} + \tilde{m}_{xy}^{h} \sqrt{m_z^h}},$$

where m_{DOS} is the temperature dependent density of states mass for holes [5]. In the classical limit (flat bands), this ensures similarity of the quantum-mechanical solution and the solution provided by a classical simulation.

Eq. (4) does not take into account any density contributions of states above E_{max}. For these states, we add a classical density correction

$$n^{add}(E_{max}) = \sum_{\nu} \frac{kT m_{xy}^{\nu} \sqrt{2 m_z^{\nu}}}{\hbar^3 \pi^2} \left[\frac{\sqrt{kT\pi}}{2} \mathrm{erfc} \sqrt{\frac{E_{max} - E_{be}}{kT}} \exp\left(\frac{E_f - E_{be}}{kT} \right) + \sqrt{E_{max} - E_{be}} \exp\left(\frac{E_f - E_{max}}{kT} \right) \right]$$

for $E_{max} > E_{be}$, where E_{be} is the energy of the band edge. For $E_{max} = E_{be}$, the formula reduces to the classical formula for the density, which can also be used for $E_{max} < E_{be}$.

To feed the Schrödinger results back to the classical device simulator, we introduce a "quantum intrinsic density", separately for electrons and holes,

$$n_i^{e,h}(z) = n_i n_{qm}^{e,h} / n_{cl}^{e,h},$$

where n_i is the classical effective intrinsic density, and n_{qm} and n_{cl} are the carrier densities computed quantum-mechanically and classically, respectively, for the same quasi Fermi potential and electrostatic potential. The quantum intrinsic densities replace the intrinsic density in various places. This method is conceptually the same as the one used by van Dort *et al.* [6], who modified n_i directly. Changing n_i directly keeps changes to the existing code to a minimum. On the other hand, introducing distinct quantum intrinsic densities for electrons and holes is more flexible and allows to treat both electrons and holes quantum-mechanically at the same time.

3 Numerical procedure

We solve the eigenvalue problem $H\Psi = E\Psi$ by guessing some value for E and inserting it in the Schrödinger equation, thereby reducing it to a second order ordinary differential equation

(ODE). We impose boundary conditions for the wave function and its derivative at both ends of the 1D Schrödinger region and try to solve the ODE. If we can fulfill the boundary conditions, E really was an eigenenergy. Otherwise, we have to make a new guess.

We solve the ODE by approximating the solution by the analytic solution for piecewise constant potential, i.e. in the interval i with potential V_i, the wave function is approximated by

$$\Psi(z) = A_i \frac{\sin(k_i z)}{k_i} + B_i \cos(k_i z),$$

where

$$k_i = \sqrt{2m_i(E - V_i)}/\hbar^2.$$

The coefficients A_i and B_i are chosen to match the boundary conditions and the continuity conditions

$$\Psi(z_i + 0) = \Psi(z_i - 0), \tag{5}$$
$$\Psi'(z_i + 0)/m_i = \Psi'(z_i - 0)/m_{i-1} \tag{6}$$

for all points z_i at the boundary between two intervals.

We solve the ODE separately on two halves of our Schrödinger region and try to join these solutions using Eq. (5) and Eq. (6). The wave function can always be matched by rescaling one of the partial solutions. By perturbation theory it can be seen that the mismatch in the derivatives gives us a correction to our estimated value for the eigenenergy, which can be used to make a better guess in the next iteration [7].

4 Simulation results for double gated SOI MOSFETs

The above described model was integrated in the device simulator DESSIS$_{\text{-ISE}}$ [8]. We performed calculations for NMOS and PMOS SOI MOSFETs and compared the classical and quantum-mechanical threshold voltages. The model device sketched in Fig. 1 and a similar PMOS device were used assuming a gate length of 50 nm and an oxide thickness t_{ox} =3 nm.

To investigate the impact of the poly gate doping on the magnitude of the quantization effect, we performed calculations both for equally doped gates and for differently doped gates. The results are shown in Figs. 4 (for electrons) and 5 (for holes). It is seen that the difference of the threshold voltage determined classically and quantum-mechanically is larger for the case with differently doped gates than for the case with equally doped gates. This is caused by the additional confinement due to the built-in potential resulting from the work function difference between the differently doped gates (Figs. 2, 3). The large shift between the two groups of curves is caused by the different mean work function and is not considered here.

Comparing Fig. 4 with Fig. 5, we also see that quantization affects holes more strongly than electrons for the {100} substrate orientation we used. This comes from the large effective mass of the two conduction band valleys perpendicular to the Si-SiO_2 interface. This large effective mass leads to a low kinetic energy (first term on the right hand side of Eq. (1)) and therefore to a dominant contribution to the density.

Finally, due to a stronger confinement, quantization is also the more important the thinner the Si layer gets (Fig. 6).

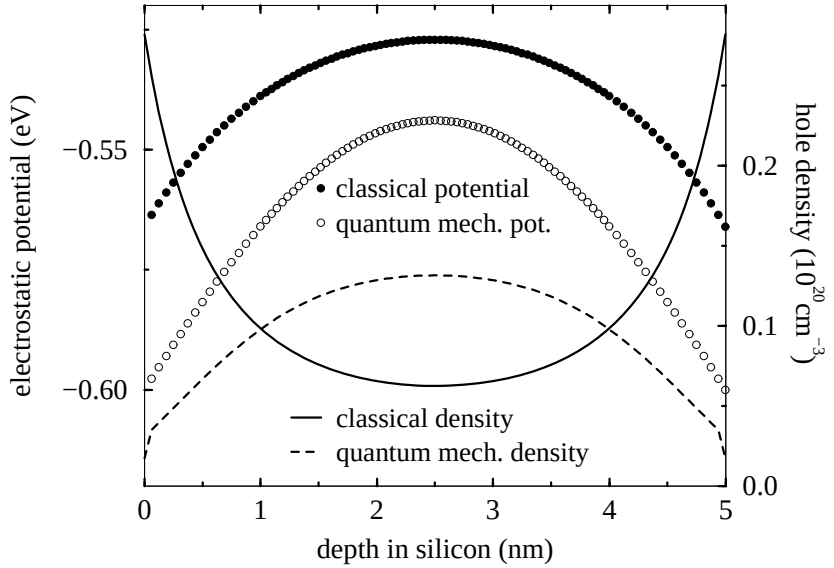

Figure 2: Hole density and electrostatic potential for a device with two p^+-poly gates ($t_{ox} = 3\,\mathrm{nm}$, $t_{Si} = 5\,\mathrm{nm}$, $N_A = 10^{15}\,\mathrm{cm}^{-3}$, T=300 K, substrate orientation {100})

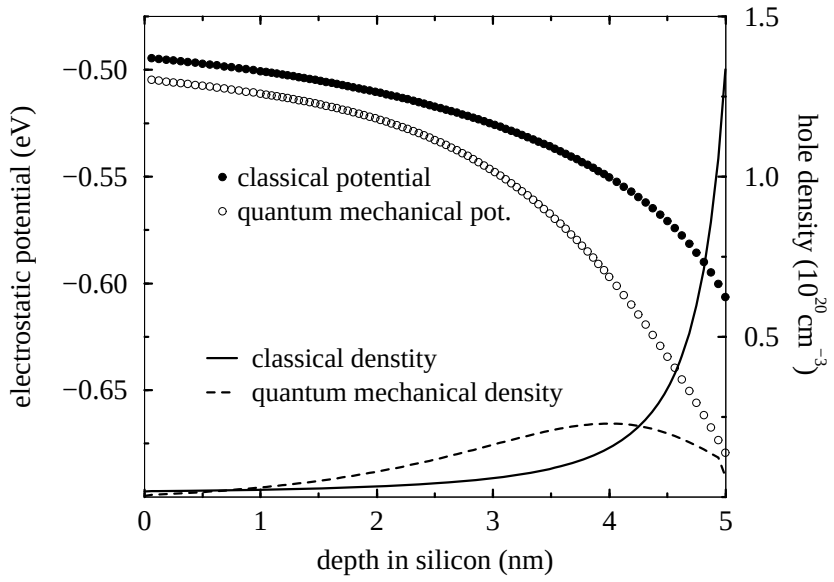

Figure 3: As Fig. 2, but for device with one n^+ and one p^+-gate.

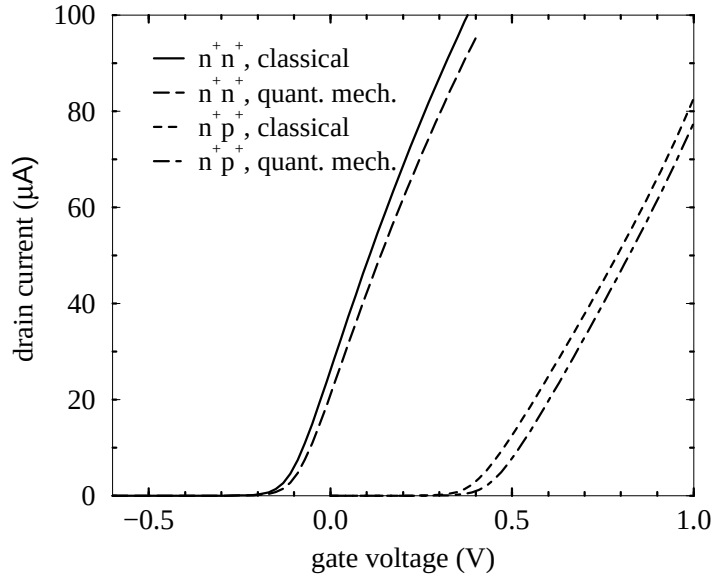

Figure 4: IV characteristics of an NMOS device computed quantum-mechanically and classically for equally and differently doped poly gates. Gate width is 1μm, all other parameters as in Fig. 2

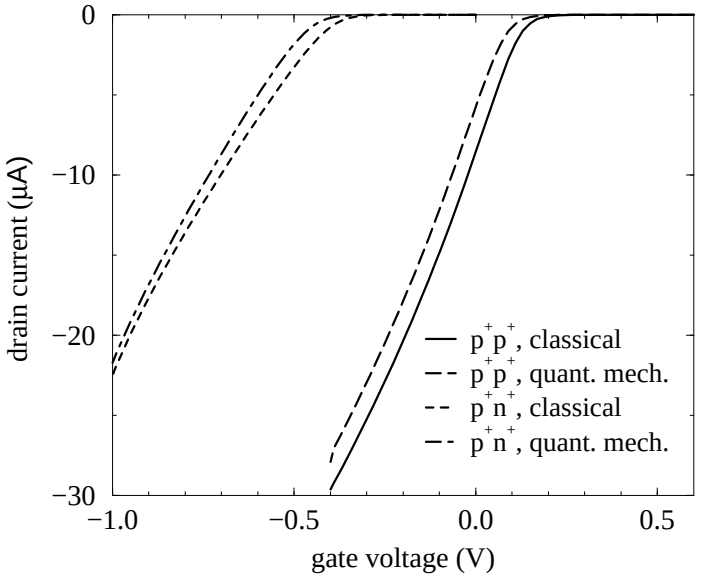

Figure 5: Similar to Fig. 4, but for PMOS device.

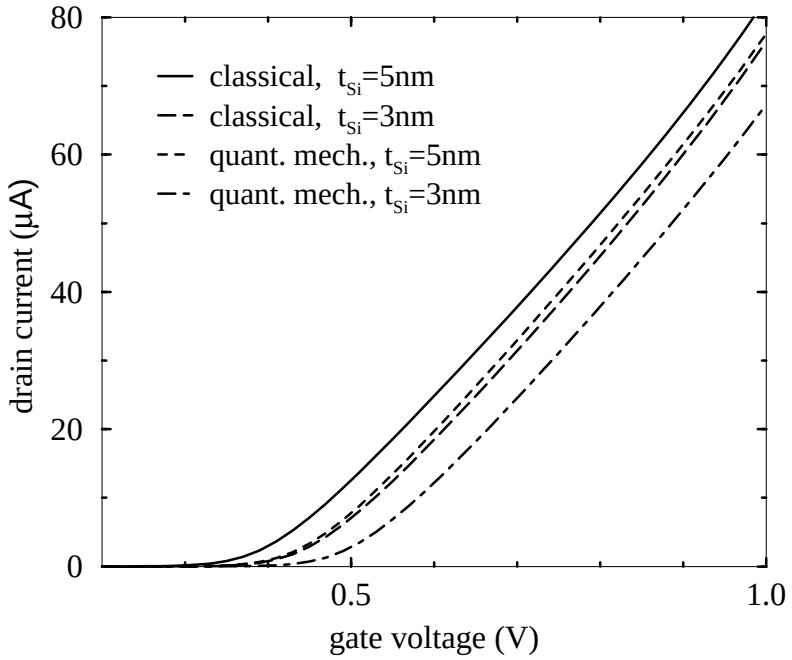

Figure 6: IV characteristics for NMOS devices with different t_{Si}. Other parameters as in Fig 2.

5 Summary

We have studied the charge carrier quantization effects in double gated SOI MOSFETs. Quantization leads to a considerable shift in the threshold voltages. The magnitude of the shift is not only a function of the silicon layer thickness, but also of carrier type and the doping of the poly gates. Specifically, the quantization effects are larger for holes than for electrons and also more pronounced for differently doped gates than for equally doped gates. Thus, an accurate model describing the effects of quantization must include all these effects.

References

[1] K. Suzuki *et al.*, in Ext. Abstracts SSDM/1994, p. 274, The Japan Society of Applied Physics, Tokyo, (1994).

[2] M. A. Green, J. Appl. Phys., 67, 2944 (1990).

[3] P. Lawaetz, Phys. Rev. B, 4, 3460 (1971).

[4] C. W. J. Benakker and H. van Houten, Solid State Physics, 44, 1 (1991).

[5] J. E. Lang, F. L. Madarasz, and P. M. Hemeger, J. Appl. Phys., 54, 3612 (1983).

[6] M. J. van Dort, P. H. Woerlee, and A. J. Walker, Solid State Electronics, 37, 411 (1994).

[7] J. M. Blatt, J. Comp. Phys., 1, 382 (1967).

[8] *DESSIS reference manual*, ISE Integrated Systems Engineering AG, 1996.